Comparing Electron Energetics and UV Brightness in Jupiter's Northern Polar Region During Juno Perijove 5

R. Ebert, T. Greathouse, G. Clark, F. Allegrini, F. Bagenal, S. Bolton, J. Connerney, G. Gladstone, M. Imai, V. Hue, et al.

▶ **To cite this version:**

R. Ebert, T. Greathouse, G. Clark, F. Allegrini, F. Bagenal, et al.. Comparing Electron Energetics and UV Brightness in Jupiter's Northern Polar Region During Juno Perijove 5. Geophysical Research Letters, 2019, 46 (1), pp.19-27. ⟨10.1029/2018GL081129⟩. ⟨hal-02367819⟩

HAL Id: hal-02367819

https://hal.science/hal-02367819v1

Submitted on 1 Sep 2021

HAL is a multi-disciplinary open access archive for the deposit and dissemination of scientific research documents, whether they are published or not. The documents may come from teaching and research institutions in France or abroad, or from public or private research centers.

L'archive ouverte pluridisciplinaire **HAL**, est destinée au dépôt et à la diffusion de documents scientifiques de niveau recherche, publiés ou non, émanant des établissements d'enseignement et de recherche français ou étrangers, des laboratoires publics ou privés.

Distributed under a Creative Commons CC BY-NC-ND 4.0 - Attribution - Non-commercial use - No Derivative Works - International License

Check for updates

AGU100 ADVANCING EARTH AND SPACE SCIENCE

Geophysical Research Letters

RESEARCH LETTER
10.1029/2018GL081129

Comparing Electron Energetics and UV Brightness in Jupiter's Northern Polar Region During Juno Perijove 5

R. W. Ebert[1,2], T. K. Greathouse[1], G. Clark[3], F. Allegrini[1,2], F. Bagenal[4], S. J. Bolton[1], J. E. P. Connerney[5], G. R. Gladstone[1,2], M. Imai[6], V. Hue[1], W. S. Kurth[6], S. Levin[7], P. Louarn[8], B. H. Mauk[3], D. J. McComas[1,9], C. Paranicas[3], J. R. Szalay[9], M. F. Thomsen[10], P. W. Valek[1], and R. J. Wilson[4]

[1]Southwest Research Institute, San Antonio, TX, USA, [2]Department of Physics and Astronomy, University of Texas at San Antonio, San Antonio, TX, USA, [3]Johns Hopkins University Applied Physics Lab, Laurel, MD, USA, [4]Laboratory for Atmospheric and Space Physics, University of Colorado Boulder, Boulder, CO, USA, [5]NASA Goddard Space Flight Center, Greenbelt, MD, USA, [6]Department of Physics and Astronomy, University of Iowa, Iowa City, IA, USA, [7]Jet Propulsion Laboratory, Pasadena, CA, USA, [8]Institut de Recherche en Astrophysique et Planétologie, Toulouse, France, [9]Department of Astrophysical Sciences, Princeton University, Princeton, NJ, USA, [10]Planetary Science Institute, Tucson, AZ, USA

Key Points:

- Simultaneous peaks are observed in electron energy flux and UV brightness when they map to same location in Jupiter's polar region at the same time
- Upward greater than downward electron energy fluxes are observed, suggesting that primary acceleration region may be below ~1.5 jovian radii
- Downward energy fluxes able to produce tens to hundreds of kilorayleigh polar UV emissions are identified; increases in energy flux due to tens of keV electrons

Correspondence to:
R. W. Ebert,
rebert@swri.edu

Citation:
Ebert, R. W., Greathouse, T. K., Clark, G., Allegrini, F., Bagenal, F., Bolton, S. J., et al. (2019). Comparing electron energetics and UV brightness in Jupiter's northern polar region during Juno perijove 5. *Geophysical Research Letters*, *46*, 19–27. https://doi.org/10.1029/2018GL081129

Received 29 OCT 2018
Accepted 20 DEC 2018
Accepted article online 26 DEC 2018
Published online 8 JAN 2019

©2018. The Authors.
This is an open access article under the terms of the Creative Commons Attribution-NonCommercial-NoDerivs License, which permits use and distribution in any medium, provided the original work is properly cited, the use is non-commercial and no modifications or adaptations are made.

Abstract We compare electron and UV observations mapping to the same location in Jupiter's northern polar region, poleward of the main aurora, during Juno perijove 5. Simultaneous peaks in UV brightness and electron energy flux are identified when observations map to the same location at the same time. The downward energy flux during these simultaneous observations was not sufficient to generate the observed UV brightness; the upward energy flux was. We propose that the primary acceleration region is below Juno's altitude, from which the more intense upward electrons originate. For the complete interval, the UV brightness peaked at ~240 kilorayleigh (kR); the downward and upward energy fluxes peaked at 60 and 700 mW/m^2, respectively. Increased downward energy fluxes are associated with increased contributions from tens of keV electrons. These observations provide evidence that bidirectional electron beams with broad energy distributions can produce tens to hundreds of kilorayleigh polar UV emissions.

Plain Language Summary Jupiter's ultraviolet (UV) aurora is produced by electrons that precipitate into the planet's atmosphere and interact with hydrogen molecules. A number of different UV auroral emission regions have been identified such as the main aurora, the aurora associated with Jupiter's satellites, and the polar aurora located poleward of the main aurora. We examine electron and UV observations from Juno in Jupiter's northern polar region to investigate the processes responsible for producing Jupiter's polar aurora. We show electrons and UV emissions having simultaneous enhancements during a time when they map to the same location of Jupiter's upper atmosphere at the same time. We present evidence that electrons with energies between 0.1 and 100 kilo electron volts (keV) are capable of producing the polar UV emissions studied here and that further acceleration of these electrons may be occurring at altitudes below the spacecraft.

1. Introduction

Jupiter's UV aurora is produced by the interaction of precipitating electrons with H_2 molecules in Jupiter's atmosphere, the UV emissions resulting from the radiative deexcitation of electronically excited states to the ground level (e.g., Broadfoot et al., 1979). A review by Grodent (2015) summarized Jupiter's UV auroral emissions as having four primary components: the (a) main emission, (b) secondary emissions equatorward of the main emission, (c) satellites footprints, and (d) polar emissions poleward of the main emission. Conjugate features are often, but not always, seen in both the northern and southern hemispheres, with some showing significant differences in emitted power (e.g., Gérard et al., 2013). This study focuses on Jupiter's northern polar UV emissions and the electrons that produce them.

Grodent et al. (2003) showed that the polar emissions contribute up to 30% of Jupiter's total auroral UV emitted power. The brightness ranges from ~0 to 10 kilorayleigh (kR) in the dark region, tens to hundreds of kilorayleighs in the swirl and active regions and dawn and midnight spots, and up to several

megarayleighs in active region polar flares (e.g., Waite et al., 2001). Prior to Juno (Bolton et al., 2017), characteristics of the electrons that produce these polar emissions were inferred from remote sensing observations. Key results include (a) the electron mean energy ranges from ~50 to 200 keV with energy fluxes up to ~20 mW/m^2 (e.g., Gustin et al., 2004, 2016); (b) that temporal variations in the polar emissions were typically associated with changes in the electron energy flux, not the mean energy (e.g., Gérard et al., 2003); and (c) the electron energy flux in the polar region was generally significantly lower than that of the main emission, with the mean energy of the precipitating electrons being comparable (Gustin et al., 2004).

Juno has provided an opportunity to make in situ measurements of the electrons in Jupiter's polar region, the region poleward of the main auroral emission, while remotely observing the polar UV emissions that they produce. Initial polar region studies have identified (a) magnetic field-aligned electron beams moving away from the planet (upward) with peaked energy distributions having characteristic energies between 20 and 400 keV (Clark et al., 2017; Ebert et al., 2017); (b) upward electron beams with MeV energies (Becker et al., 2017; Bonfond et al., 2018; Mauk, Haggerty, Paranicas, et al., 2017; Paranicas et al., 2018); and (c) bidirectional (upward and downward) electron beams with broad energy distributions that begin to have a steeper slope, that is, *rollover*, between ~2 and 5 keV and have a power law tail that extends up to at least ~100 keV (Allegrini et al., 2017; Ebert et al., 2017). The downward beams (moving toward the planet) associated with these broad-in-energy electron distributions appear to be the only source of precipitating electrons at energies below 100 keV in the polar region. Analysis by Ebert et al. (2017) for two separate intervals showed that the energy flux associated with these downward beams observed between ~1.4 and 2.9 jovian radii (R_J; 1 R_J ~ 71,492 km) ranged from ~0.1 to 5 mW/m^2, which is expected to produce between ~1 and 50 kR of UV emissions.

The polar region UV emissions observed during Juno's first perijove (PJ1) showed distinct features between the north and south (Bonfond et al., 2017; Connerney, Adriani, et al., 2017). The northern polar emissions showed auroral filaments and flares in the active region and relatively faint, patchy emissions in the swirl region. Most of the southern polar region was devoid of emissions except for a bright emission feature extending from the nightside flank of the main emission and a bright arc parallel to the main emission (Connerney, Adriani, et al., 2017; Bonfond et al., 2017). Polar UV emissions up to a few hundreds of kilorayleighs were observed along Juno's footpath during PJ1 (Bonfond et al., 2017). The question of whether the electron beams described above could produce these brighter polar UV emissions remains unanswered.

In this letter, we analyze electron and UV observations in Jupiter's northern polar region during Juno perijove 5 (PJ5) on day of year (DOY) 86, 2017. We focus on a period between 08:00:00 and 08:36:00 UT when Juno ranged between 89°–46°N in jovigraphic latitude and 1.95–1.18 R_J in jovicentric radial distance, a period where both electrons and UV emissions are observed. Specifically, we examine the electron distributions along magnetic field lines that map to UV emissions in Jupiter's upper atmosphere and determine whether the energy flux associated with the downward electrons can account for the UV brightness observed by Juno in Jupiter's northern polar region during this timeframe.

2. Instruments and Data Sets

We focus on electron observations from Juno's Jovian Auroral Distributions Experiment Electron (JADE-E) sensors (McComas et al., 2017) and Jupiter Energetic particle Detector Instrument (JEDI; Mauk, Haggerty, Jaskulek, et al., 2017) along with observations of ultraviolet emissions from Juno's Ultraviolet Spectrograph (UVS; Gladstone et al., 2017). JADE-E consists of two nearly identical sensors (E060 and E180) designed to measure the energy and pitch angle distribution of ~0.1–100-keV electrons in Jupiter's polar magnetosphere. A third sensor (E300) was turned off due to a high-voltage power supply failure. Each sensor covers 120° in azimuth (Juno's spin plane) and has deflectors that track the direction of the magnetic field up to ±35° in elevation (up to 40 keV; ~ ±15° at 100 keV) when operating in high-rate science mode. The deflection angles are calculated using magnetic field vectors received from the Juno magnetometer (Connerney, Benn, et al., 2017). The angular resolution is ~7.5° in azimuth and ~2–5.5° in elevation. The pitch angle resolution is 7.5°. Due to the E300 sensor being off, JADE-E has full pitch angle coverage for ~1/3 of every ~30-s spacecraft spin period but covers at least 120° at all times including either the upward or downward magnetic field-aligned direction. The JADE data presented here have a 1-s time resolution.

JEDI is composed of three mounted (nonmoving) sensors. Two of the sensors (j90 and j270) are optimized to measure magnetic field-aligned energetic ions and electrons over Jupiter's auroral regions and thus have their field of views primarily in Juno's spin plane. The third sensor (j180) is mounted such that it essentially observes the full sky once every 30 s or one spacecraft rotation. Energetic electrons (~25 to >800 keV) are measured by 500-μm-thick solid-state detectors that are flashed with 2 μm of aluminum to prevent less than 250-keV ions from penetrating. When observations from all three sensors are combined in its high-rate mode, the full pitch angle distribution can be resolved on an ~1-s cadence over the auroral regions.

Juno UVS is an imaging spectrograph sensitive to wavelengths between 68 and 210 nm. It observes Jupiter's northern and southern auroras for several hours during each Juno perijove pass from jovicentric distances of ~1.3–7 R_J. UVS is oriented such that its 7.5° long dog-bone-shaped slit is pointed nominally perpendicular to the spin plane (Greathouse et al., 2013). A scan mirror allows the field of view to be directed ±30° relative to the spin plane giving UVS access to half the sky at any given spacecraft orientation. This enables UVS to observe a large number of bright UV stars to calibrate the instrument (Hue et al., 2018). UVS observes the jovian aurora in a series of 30-s scans. The data along with reconstructed SPICE kernels are used to produce scan maps of Jupiter's UV auroral emissions. The UV brightness is determined by integrating the emissions between 115–118 and 125–165 nm and then multiplying by 2.5 (J. C. Gérard, personal communication) to estimate the total H_2 emission between 75 and 198 nm.

3. Electron and UV Observations in Jupiter's Northern Auroral Region

Figure 1 is an overview of the UVS and JADE observations in Jupiter's northern auroral region on DOY 86, 2017, just prior to Juno PJ5. The UVS brightness and color ratio observations shown in Figures 1a and 1b, respectively, are a composite of images obtained between 08:16 and 08:18 UT. These images are made up of three spatially adjacent scans of Jupiter's auroral region and represent only a small subset of the UV observations obtained from Juno's northern polar pass during PJ5. Juno's magnetic foot point, predicted using the JRM09 model for Jupiter's magnetic field (Connerney et al., 2018), is superimposed on each figure. Juno's trajectory during this period traversed the dayside of Jupiter's northern polar region, the main emission, and the Io footprint tail (IFPT). The white circles on the trajectory identify Juno's magnetic footprint at the time the UV observations were collected.

The polar region UV emissions include a diffuse patch of emissions at ~75°N latitude and 180° west longitude with a brightness of ~130 kR, a circular emission feature between ~62° and 68°N latitude with a brightness of ~100–240 kR around its perimeter and a relatively dark center region, and an ~100–120-kR arc at ~60°N latitude, and ~160–175° west longitude. These polar UV emissions, and the electrons that produce them, are the focus of this study.

The region of the main emission where Juno crossed had a peak brightness of ~650 kR at the imaged time of 8:16–8:18 UT and was observed between ~50 and 60°N latitude. The narrow arc equatorward of the main emission is the IFPT. The color ratio of the UV emissions, defined as the ratio between the integrated brightness from 158 and 162 nm and 126 and 130 nm, is used to estimate the energy and penetration depth of the precipitating electrons. The color ratio ranged from 10 to 20 for the diffuse and circular emission features in the polar region and the poleward edge of the main emission, suggesting that the electrons producing these emissions have a large penetration depth. The color ratio for the polar region arc, the equatorward edge of the main emission, and the IFPT emissions is <5, suggesting that these emissions are produced by less energetic electrons that do not penetrate as deep into Jupiter's atmosphere.

Figures 1c–1f show the JADE-E electron observations from 08:00 to 08:36 UT on DOY 086, 2017, a period when Juno ranged from 89–46°N in jovigraphic latitude and 1.95–1.18 R_J in jovicentric radial distance. For most of this interval, Juno traversed Jupiter's northern polar region before crossing the main emission at approximately 08:29:45 UT. Energy-time differential energy flux spectrograms of upward and downward 0.1–100-keV electrons are shown in Figures 1c and 1d, respectively. The electron pitch angle distributions are shown in Figure 1e, and the upward and downward electron energy fluxes are shown in Figure 1f.

Except for a narrow beam of upward electrons at ~08:06:00 UT, the electron observations between ~08:00 and 08:18 UT are characterized by penetrating radiation, identified as the narrow vertical bands of spin-modulated signal across all energy steps in the energy-time spectrograms shown in Figures 1b and 1c, and

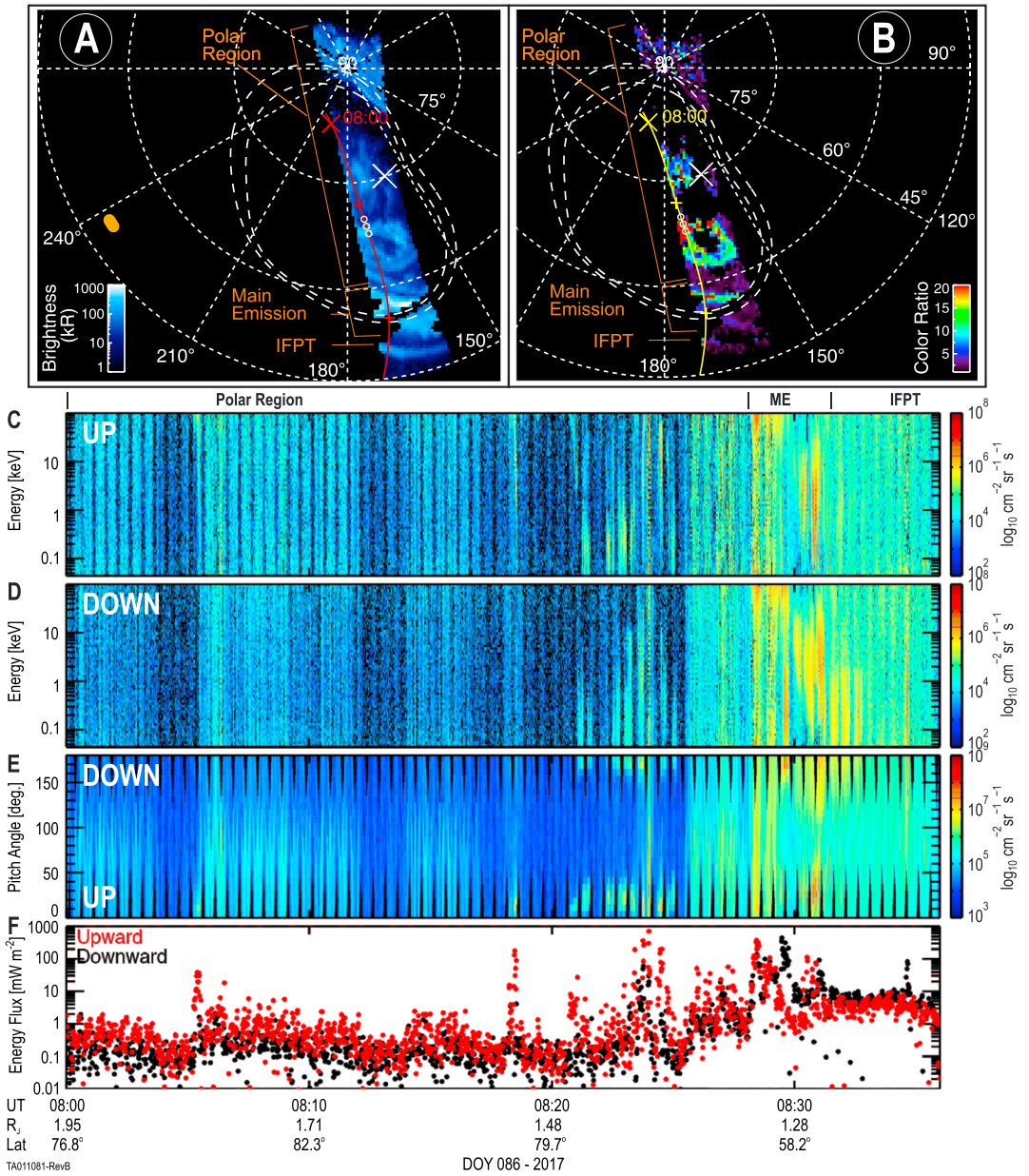

Figure 1. (a) UV brightness and (b) color ratio observations of Jupiter's northern polar region, main emission (ME), and Io footprint tail (IFPT) collected between 08:16 and 08:18 UT on DOY 86, 2017, during Juno perijove 5. Red (left) and yellow (right) lines denote Juno's trajectory based on the JRM09 magnetic field model (Connerney et al., 2018). White circles indicate when the images were collected. White X identifies the magnetic pole. Orange elongated dot marks the Sun's position. Ovals denoted by the white dashed lines represent the statistical boundaries of Jupiter's main auroral emission (Bonfond et al., 2012). (c and d) Energy-time differential energy flux spectrograms of upward and downward 0.1–100-keV electrons observed along Juno's trajectory shown in Figure 1a between 08:00 and 08:36 UT. (e) Pitch angle-time differential energy flux spectrograms for 0.1–100-keV electrons. (f) Upward (red) and downward (black) energy fluxes of 0.1–100-keV electrons. Uncertainties in the energy flux range up to ~30%, the largest uncertainties being associated with values below 1 mW/m^2.

regions where the signal is near the noise floor of the instrument, that is, the one count level. The penetrating radiation, that is, particles outside of JADE's nominal energy range, has been identified by other instruments as upward beams of MeV electrons in Jupiter's polar region (e.g., Becker et al., 2017; Bonfond et al., 2018; Mauk, Haggerty, Paranicas, et al., 2017; Paranicas et al., 2018). At 08:18:15 UT, JADE-E observed beams of upward and downward (bidirectional) electrons with energy fluxes up to ~175 and ~4 mW/m^2,

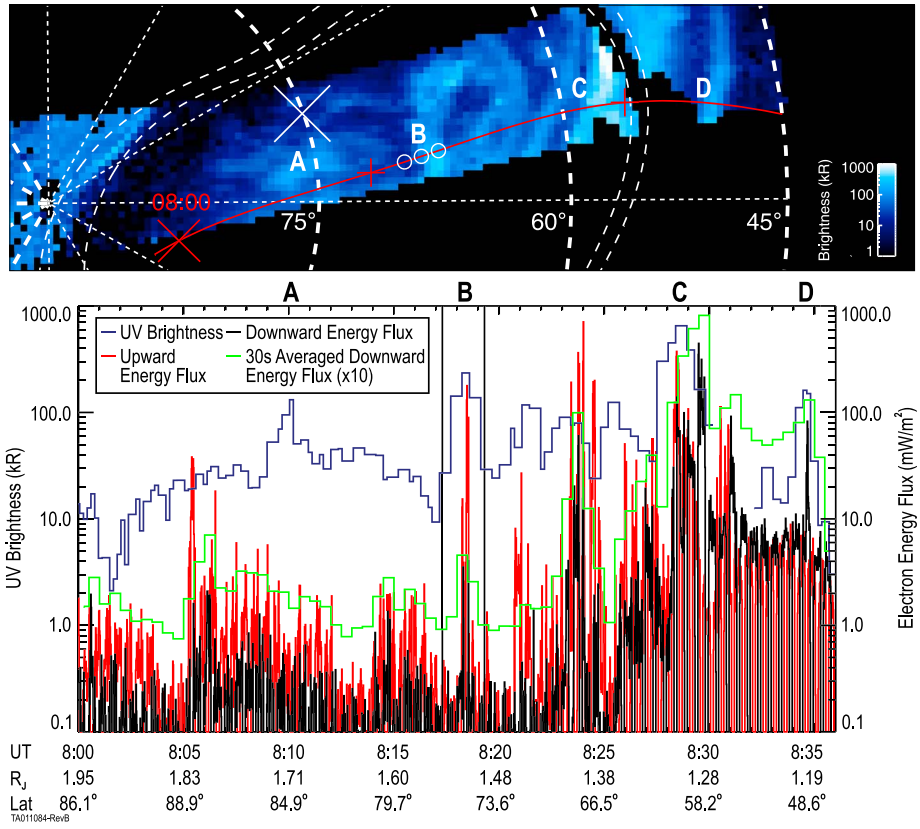

Figure 2. (Top) UV brightness observations in Jupiter's northern auroral region during the same period described in Figure 1. Red line denotes Juno's trajectory. White circles identify when the image was taken. Red crosses denote 15-min tick marks. (Bottom) Time series of upward (red curve) and downward (black curve) electron energy flux between 08:00 and 08:36 UT on DOY 86, 2017. Green curve denotes a time series of 30-s averaged downward energy flux multiplied by a factor of 10. Blue curve shows the UV brightness measured between 08:16 and 08:18 UT that map to the same regions of Jupiter's upper atmosphere as the electrons. Black vertical lines bound the period when the electrons and UV emissions are observed at the same time. Labels A, B, C, and D identify UV brightness features in the top panel associated with the UV brightness peaks in the bottom panel.

respectively. Between ~08:18:15 and 08:25:30 UT, JADE-E continued to observe bidirectional electron beams in the polar region. The downward electrons had pitch angles within ~22.5° of Jupiter's magnetic field (based on a pitch angle bin size of 7.5°) and had energy fluxes from <1 to 60 mW/m^2. The angular extent of the geometric magnetic loss cone at Juno's location ranged from ~30° to 40° during this period. The upward beams are within ~30–40° of Jupiter's magnetic field with energy fluxes up to ~240 mW/m^2. The timing of these observations coincided with Juno being magnetically connected to the circular UV and polar arc emission features described above, UV emissions that are observed to last for several minutes.

At ~08:25:30 UT, Juno crossed into a region of enhanced penetrating radiation. A step-wise increase in the JADE background counts is observed at this time (not shown). This enhanced radiation is also observed by Juno UVS (Bonfond et al., 2018). Juno crossed the main emission at starting ~08:29:45 UT and the IFPT at ~08:35:00 UT. The radiation environment remained enhanced through 08:36:00 UT. Details of the electron distributions observed by JADE over the main emission and IFPT are found in Allegrini et al. (2017) and Szalay et al. (2017, 2018).

Figure 2 compares the UV brightness and electron energy flux along Juno's trajectory for the period described in Figure 1. Figure 2 (top) is a zoomed in view of the UV brightness image shown in Figure 1a. Figure 2 (bottom) shows a time series of upward and downward electron energy fluxes measured by JADE-E between 08:00 and 08:36 UT, observations which magnetically map to specific latitudes and longitudes in Jupiter's upper atmosphere along Juno's trajectory. UV brightness measurements, collected between 8:16 and 8:18 UT, that map to the same latitudes and longitudes are also shown. The black

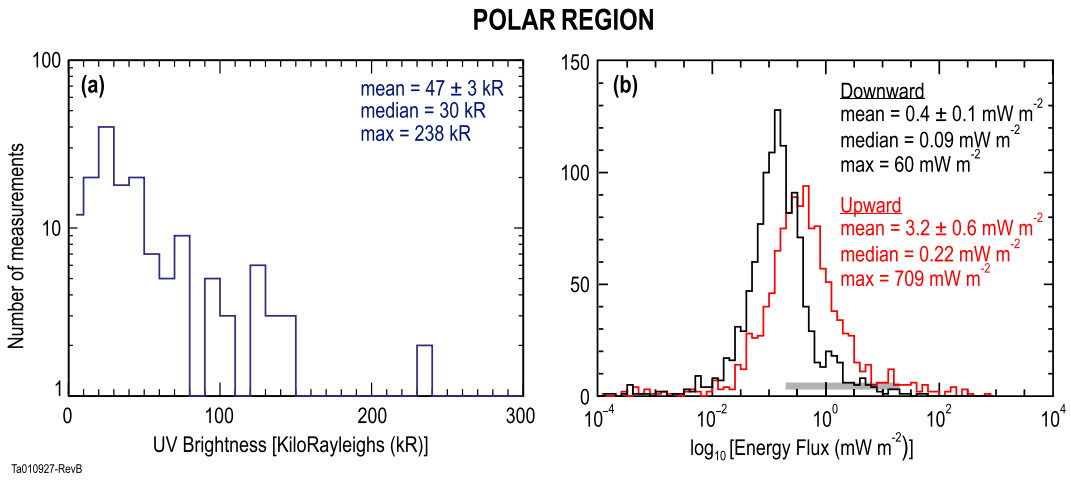

Figure 3. (a) Distributions of UV brightness and (b) upward and downward electron energy fluxes in Jupiter's polar region for the observations in the bottom panel of Figure 2. The black shaded bar in Figure 3b identifies downward energy flux values that could produce the range of UV brightness in Figure 3a. Observations associated with the main emission and Io footprint tail were not included in this figure.

vertical lines bound the period when the electron energy flux and UV brightness are observed simultaneously. The energy fluxes between 08:00 and 08:15 UT are measured 1–16 min earlier than the UV emissions, while the energy fluxes between 08:19 and 08:36 UT are measured 1–17 min later than the UV emissions.

The UV brightness profile in Figure 2 (bottom) has several peaks corresponding to emission features in the image shown in Figure 2 (top). The electron energy fluxes also show several peaks, some corresponding to peaks in the UV brightness. At the time the UV observations are collected, identified by the period bounded by the black vertical lines, Juno was magnetically connected to a polar UV emission feature with a brightness of ~240 kR. Interestingly, the downward and upward electron energy fluxes also showed a peak during this time. The downward energy flux is ~ 4 mW/m^2, while the upward energy flux is to ~175 mW/m^2. Based on the factor of 10 conversion between electron energy flux and UV brightness (1 mW/m^2 ~ 10 kR) described in Grodent et al. (2001), the downward energy flux observed by JADE-E is likely not sufficient to produce the UV brightness observed during this time, while the upward energy flux is near the needed value. There is little evidence of a contribution from the >100-keV electrons observed by JEDI at this time. A time series of 30 s averaged downward energy flux values multiplied by a factor of 10 are shown for direct comparison with the UV brightness. We note that the energy flux estimates at ~08:24 UT and after ~08:25:30 UT likely have a contribution from penetrating radiation. Implications of these observations are discussed in section 4.

The electron energy fluxes also peaked when Juno crossed the main emission and the IFPT, as predicted using the JRM09 magnetic field model. We interpret this as evidence that the JRM09 model is doing a good job of mapping Juno's magnetic footprint to Jupiter's upper atmosphere during these times. The correlation between the electron energy flux and UV brightness is not as clear throughout the rest of the polar region. This is likely due to the time difference between when the UV and electron observations were obtained and the variable nature of the electron distributions and the UV emissions in the polar region, which can change on timescales of seconds to minutes. This is less of an issue with the main auroral and IFPT emissions since they are longer-lived features.

Figure 3 shows the distribution of UV brightness and downward and upward energy fluxes for the polar region observations in the bottom panel of Figure 2. The UV brightness ranged between 2 and 238 kR and had mean and median values of 47 and 30 , respectively. Based on Grodent et al. (2001), downward electron energy fluxes ranging between 0.2 and 24 mW/m^2 with a mean value of ~5 mW/m^2 are required to produce these UV emissions. The downward energy fluxes measured by JADE-E had mean and median values of 0.4 and 0.09 mW/m^2 with 20% of the values being greater than 0.2 mW/m^2 up to a maximum of 60 mW/m^2. This indicates that a subset of the downward electron energy fluxes observed here could produce the range of UV brightness identified in Figure 3a. The upward energy fluxes are far greater than the downward energy

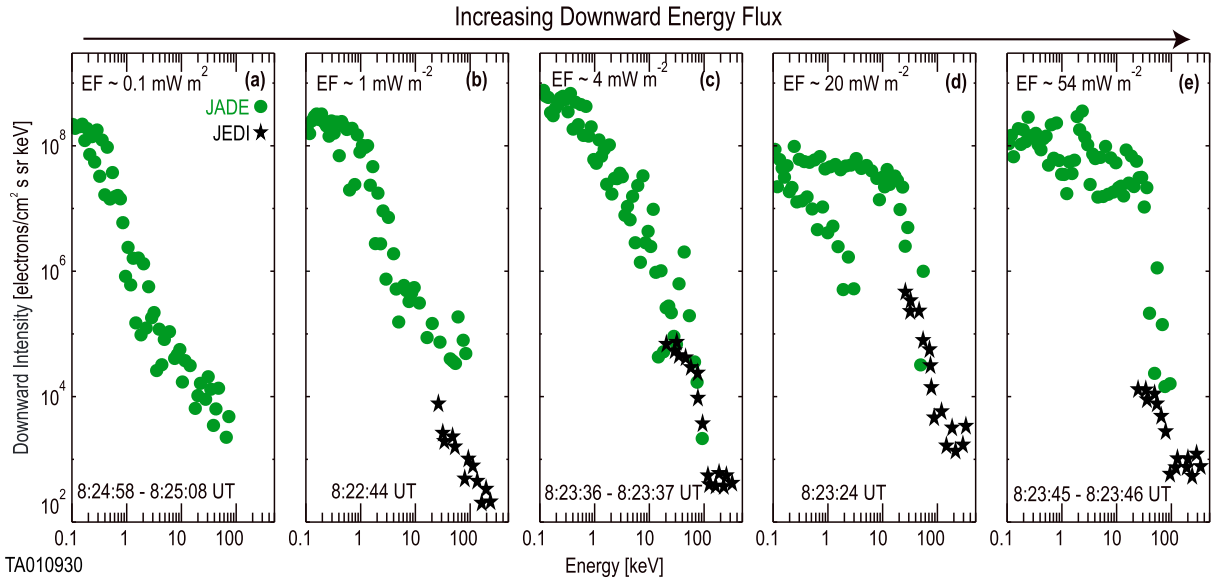

Figure 4. Energy spectra of 0.1–500-keV downward electrons observed over Jupiter's northern polar region for selected periods from the interval between ~08:22:30 and 08:25:30 UT in the bottom panel of Figure 2. The pitch angle range of these distributions is between ~150° and 180°. Green circles and black stars represent the JADE and JEDI observations, respectively. These electrons distributions are ordered, from left to right, by increasing downward energy flux.

fluxes, a common feature observed by Juno in Jupiter's polar region that is interpreted as a real spatial and temporal effect (Ebert et al., 2017; Mauk, Haggerty, Paranicas, et al., 2017). We return to this fact in the discussion.

Figure 4 combines JADE and JEDI observations to examine the energy spectra of downward electrons with energies from 0.1 to 500 keV for distributions having different energy flux values. The pitch angle range of these distributions is between ~150° and 180°. A majority of the electrons have energies below 100 keV during this interval. The energy flux value associated with each distribution increases from left to right. The energy spectra in Figures 4a–4c start to steepen or roll over at or below 1 keV, while the energy spectra in Figures 4d and 4e steepen between ~20 and 50 keV. The variability in the electron intensities shown in Figures 4d and 4e is a result of the fine structure and temporal variability of these electron distributions. For cases where the electron beam is observed for <1 s, it is possible that adjacent energy steps can observe very different intensities due to the manner in which JADE-E sweeps over its energy range (Allegrini et al., 2017). These observations indicate that the distributions of downward electrons with increased energy flux discussed here are driven by increased contributions from a few to a few tens of keV electrons.

4. Discussion and Summary

We present a quantitative comparison of electron energy flux and UV brightness in Jupiter's northern polar region, the region poleward of Jupiter's main emission, prior to Juno's perijove 5. We focus on a 36-min interval along Juno's trajectory where electrons and polar UV emissions map to the same region of Jupiter's upper atmosphere. This includes a 2-min period when they are both observed simultaneously and peaks in the UV brightness and upward and downward electron energy fluxes are identified. Juno is at a jovicentric distance of ~1.50 R_J and a jovigraphic latitude of ~75° during these simultaneous observations.

Magnetically mapping the Juno electron and UV observations to Jupiter's upper atmosphere is performed using the JRM09 magnetic field model (Connerney et al., 2018). The mapping appeared to do a reasonable job as evidenced by the peaks in the electron energy flux when Juno is predicted to cross the main auroral and Io footprint tail emissions. In the polar region, identifying simultaneous electron and UV observations from Juno that map to the same region of Jupiter's upper atmosphere is challenging. This is due to the rapid rate at which Juno traverses the polar region (several tens of km/s), the subsecond to few minute variability in both the polar region electron distributions and UV emissions (e.g., Gérard et al., 2003), and the fact that

UVS observes only a slice of Jupiter's auroral region for only small fraction of each 30-s scan, never observing the same region for more than a few consecutive scans (Gladstone et al., 2017).

The downward energy flux at Juno's altitude during the simultaneous observations described above is not sufficient to generate the observed UV brightness, while the upward energy flux is near the value needed to produce these emissions. Upward greater than downward energy flux is a common feature in the polar region at the altitudes that Juno has explored (Ebert et al., 2017; Mauk, Haggerty, Jaskulek, et al., 2017). This feature has also been observed at Earth in auroral structures associated with Alfvénic activity (e.g., Li et al., 2013). There, observations of intense upward fluxes of low-energy (broadband) electrons in these regions has been interpreted as evidence of acceleration below the spacecraft where the dissipation of intense downward Poynting flux leads to an increase in downward energy flux at lower altitudes (Li et al., 2013). We consider this a possible explanation for the polar region energy flux observations presented here, the primary acceleration region being closer to Jupiter, the more intense upward distributions observed at Juno's altitude escaping from that region. Electron acceleration below ~2.5 R_J has also been suggested as a source of the electron conics observed by Juno/JADE in regions of radio wave generation (Louarn et al., 2018).

Over the complete polar region interval considered here, Juno decreased from ~1.95 to 1.3 R_J in jovicentric radial distance. The UV brightness ranged from 2 to 240 kR (requiring ~0.2–24 mW/m^2 of downward energy flux), while the energy flux associated with the downward and upward electrons ranged from <1–60 and <1–700 mW/m^2, respectively. This suggests that a subset of the downward energy fluxes observed here can produce the range of UV brightness identified in Figure 3a, providing evidence that bidirectional electron beams having broad energy distributions are capable of producing tens to hundreds of kilorayleigh polar UV emissions. The distributions of downward electrons with increased energy flux described here are driven by increased contributions from a few to a few tens of keV electrons. This differs from interpretations based on temporal variations of UV observations from HST where increased downward energy fluxes in the polar region were attributed to an increase in electron number flux or intensity (e.g., Gérard et al., 2003).

Acknowledgments
This work was supported as a part of the work on the Jovian Auroral Distributions Experiment (JADE) and Juno Ultraviolet Spectrograph (Juno UVS) on NASA's Juno mission. The JNO-J/SW-JAD-3-CALIBRATED-V1.0 and JNO-SS-3-FGM-CALIBRATED-V1.0 data sets were obtained from the Planetary Data System (PDS) at http://pds.nasa.gov/. The Jovian Energetic particle Detector Instrument (JEDI) work was funded by NASA's New Frontiers Program for Juno via a subcontract with the Southwest Research Institute. The JEDI data presented here reside at the PDS. The research at the University of Iowa was supported by NASA through contract 699041X with the Southwest Research Institute. R. W. E. would like to thank Rene Limon for support with graphics.

References

Allegrini, F., Bagenal, F., Bolton, S., Connerney, J., Clark, G., Ebert, R. W., et al. (2017). Electron beams and loss cones in the auroral regions of Jupiter. *Geophysical Research Letters*, *44*, 7131–7139. https://doi.org/10.1002/2017GL073180

Becker, H. N., Santos-Costa, D., Jørgensen, J. L., Denver, T., Adriani, A., Mura, A., et al. (2017). Observations of MeV electrons in Jupiter's innermost radiation belts and polar regions by the Juno radiation monitoring investigation: Perijoves 1 and 3. *Geophysical Research Letters*, *44*, 4481–4488. https://doi.org/10.1002/2017GL073091

Bolton, S. J., Lunine, J., Stevenson, D., Connerney, J. E. P., Levin, S., et al. (2017). The Juno mission. *Space Science Reviews*, *213*(1–4), 5–37. https://doi.org/10.1007/s11214-017-0429-6

Bonfond, B., Gladstone, G. R., Grodent, D., Gérard, J. C., Greathouse, T. K., Hue, V., et al. (2018). "Bar code" events in the Juno-UVS data: Signature ~10 MeV electron microbursts at Jupiter. *Geophysical Research Letters*, *45*, 12,108–12,115. https://doi.org/10.1029/2018GL080890

Bonfond, B., Gladstone, G. R., Grodent, D., Greathouse, T. K., Versteeg, M. H., Hue, V., et al. (2017). Morphology of the UV aurorae Jupiter during Juno's first perijove observationsn. *Geophysical Research Letters*, *44*, 4463–4471. https://doi.org/10.1002/2017GL073114

Bonfond, B., Grodent, D., Gérard, J. C., Stallard, T., Clarke, J. T., Yoneda, M., et al. (2012). Auroral evidence of Io's control over the magnetosphere of Jupiter. *Geophysical Research Letters*, *39*, L01105. https://doi.org/10.1029/2011GL050253

Broadfoot, A. L., Belton, M. J., Takacs, P. Z., Sandel, B. R., Shemansky, D. E., Holberg, J. B., et al. (1979). Extreme ultraviolet observations from Voyager 1 encounter with Jupiter. *Science*, *204*(4396), 979–982. https://doi.org/10.1126/science.204.4396.979

Clark, G., Mauk, B. H., Haggerty, D., Paranicas, C., Kollmann, P., Rymer, A., et al. (2017). Energetic particle signatures of magnetic field-aligned potentials over Jupiter's polar regions. *Geophysical Research Letters*, *44*, 8703–8711. https://doi.org/10.1002/2017GL074366

Connerney, J. E. P., Adriani, A., Allegrini, F., Bagenal, F., Bolton, S. J., Bonfond, B., et al. (2017). Jupiter's magnetosphere and aurorae observed by the Juno spacecraft during its first polar orbits. *Science*, *356*(6340), 826–832. https://doi.org/10.1126/science.aam5928

Connerney, J. E. P., Benn, M., Bjarno, J. B., Denver, T., Espley, J., Jorgensen, J. L., et al. (2017). The Juno magnetic field investigation. *Space Science Reviews*, *213*(1-4), 39–138. https://doi.org/10.1007/s11214-017-0334-z

Connerney, J. E. P., Kotsiaros, S., Oliversen, R. J., Espley, J. R., Joergensen, J. L., Joergensen, P. S., et al. (2018). A new model of Jupiter's magnetic field from Juno's first nine orbits. *Geophysical Research Letters*, *45*(6), 2590–2596. https://doi.org/10.1002/2018GL077312

Ebert, R. W., Allegrini, F., Bagenal, F., Bolton, S. J., Connerney, J. E. P., Clark, G., et al. (2017). Spatial distribution and properties of 0.1–100 keV electrons in Jupiter's polar aurora region. *Geophysical Research Letters*, *44*, 9199–9207. https://doi.org/10.1002/2017GL075106

Gérard, J.-C., Grodent, D., Radioti, A., Bonfond, B., & Clarke, J. T. (2013). Hubble observations of Jupiter's north-south conjugate ultraviolet aurora. *Icarus*, *226*(2), 1559–1567. https://doi.org/10.1016/j.icarus.2013.08.017

Gérard, J.-C., Gustin, J., Grodent, D., Clarke, J. T., & Grard, A. (2003). Spectral observations of transient features in the FUV Jovian polar aurora. *Journal of Geophysical Research*, *108*(A8), 1319. https://doi.org/10.1029/2003JA009901

Gladstone, G. R., Persyn, S. C., Eterno, J. S., Walther, B. C., Slater, D. C., Davis, M. W., et al. (2017). The ultraviolet spectrograph on NASA's Juno mission. *Space Science Reviews*, *213*(1-4), 447–473. https://doi.org/10.1007/s11214-014-0040-z

Greathouse, T. K., G. R. Gladstone, M. W. Davis, D. C. Slater, M. H. Versteeg, K. B. Persson, et al. (2013), Performance results from in-flight commissioning of the Juno Ultraviolet Spectrograph (Juno-UVS).

Grodent, D. (2015). A brief review of ultraviolet auroral emissions on giant planets. *Space Science Reviews*, *187*, 23–50.

Grodent, D., Clarke, J. T., Waite, J. H. Jr., Cowley, S. W. H., Gérard, J.-C., & Kim, J. (2003). Jupiter's polar aurora emissions. *Journal of Geophysical Research*, *108*(A10), 1366. https://doi.org/10.1029/2003JA010017

Grodent, D., Waite, J. H. Jr., & Gérard, J.-C. (2001). A self-consistent model of the Jovian auroral thermal structure. *Journal of Geophysical Research*, *106*(A7), 12,933–12,952. https://doi.org/10.1029/2000JA900129

Gustin, J., Feldman, P. D., Gérard, J.-C., Grodent, D., Vidal-Madjar, A., Ben Jaffel, L., et al. (2004). Jovian auroral spectroscopy with FUSE: Analysis of self-absorption and implications for electron precipitation. *Icarus*, *171*(2), 336–355. https://doi.org/10.1016/j.icarus.2004.06.005

Gustin, J., Grodent, D., Ray, L. C., Bonfond, B., Bunce, E. J., Nichols, J. D., & Ozak, N. (2016). Characteristics of north Jovian aurora form STIS FUV spectral images. *Icarus*, *268*, 215–241. https://doi.org/10.1016/j.icarus.2015.12.048

Hue, V., Kammer, J., Gladstone, G. R., Greathouse, T. K., Davis, M. W., Bonfond, B., et al. (2018). In-flight characterization and calibration of the Juno-Ultraviolet Spectrograph (Juno-UVS), Proceedings of SPIE, 10699, 1069931. https://doi.org/10.1117/12.2311563

Li, B., Marklund, G., Karlsson, T., Sadeghi, S., Lindqvist, P. A., Vaivads, A., et al. (2013). Inverted-V and low-energy broadband electron acceleration features of multiple auroras within a large-scale surge. *Journal of Geophysical Research: Space Physics*, *118*, 5543–5552. https://doi.org/10.1002/jgra.50517

Louarn, P., Allegrini, F., McComas, D. J., Valek, P. W., Kurth, W. S., André, N., et al. (2018). Observation of electron conics by Juno: Implications for radio generation and acceleration processes. *Geophysical Research Letters*, *45*, 9408–9416. https://doi.org/10.1029/2018GL078973

Mauk, B. H., Haggerty, D. K., Jaskulek, S. E., Schlemm, C. E., Brown, L. E., Cooper, S. A., et al. (2017). The Jupiter Energetic Particle Detector Instrument (JEDI) investigation for the Juno mission. *Space Science Reviews*, *213*(1-4), 289–346. https://doi.org/10.1007/s11214-013-0025-3

Mauk, B. H., Haggerty, D. K., Paranicas, C., Clark, G., Kollmann, P., Rymer, A. M., et al. (2017). Juno observations of energetic charged particles over Jupiter's polar regions: Analysis of mono and bi-directional electron beams. *Geophysical Research Letters*, *44*, 4410–4418. https://doi.org/10.1002/2016GL072286

McComas, D. J., Alexander, N., Allegrini, F., Bagenal, F., Beebe, C., Clark, G., et al. (2017). The Jovian Auroral Distributions Experiment (JADE) on the Juno mission to Jupiter. *Space Science Reviews*, *213*(1-4), 547–643. https://doi.org/10.1007/s11214-013-9990-9

Paranicas, C., Mauk, B. H., Haggerty, D. K., Clark, G., Kollmann, P., Rymer, A. M., et al. (2018). Intervals of intense energetic electron beams over Jupiter's poles. *Journal of Geophysical Research: Space Physics*, *123*, 1989–1999. https://doi.org/10.1002/2017JA025106

Szalay, J. R., Allegrini, F., Bagenal, F., Bolton, S., Clark, G., et al. (2017). Plasma measurements in the Jovian polar region with Juno/JADE. *Geophysical Research Letters*, *44*, 7122–7130. https://doi.org/10.1002/2017GL072837

Szalay, J. R., Bonfond, B., Allegrini, F., Bagenal, F., Bolton, S., Clark, G., et al. (2018). Juno observations connected to the Io footprint tail aurora. *Journal of Geophysical Research: Planets*, *123*, 3061–3077. https://doi.org/10.1029/2018JE005752

Waite, J. H. Jr., Gladstone, G. R., Lewis, W. S., Goldstein, R., McComas, D. J., Riley, P., et al. (2001). An auroral flare at Jupiter. *Nature*, *410*(6830), 787–789. https://doi.org/10.1038/35071018